NSG-117

Oxide Growth in a Al-Al_2O_3 SAP-Type Alloy by Hot Stage Transmission Electron Microscopy

By

R. Natesh[1]

and

G. S. Ansell[2]

Interdisciplinary Materials Research Center

Rensselaer Polytechnic Institute

Troy, New York

SUBMITTED TO
ACTA METALLURGICA

1. Formerly at Rensselaer Polytechnic Institute, now at the Applied Research Laboratory, U. S. Steel Corporation, Monroeville, Pennsylvania.

2. Professor of Metallurgical Engineering, Rensselaer Polytechnic Institute, Troy, New York.

ABSTRACT

The oxidation of an Al- 2% Al_2O_3 SAP-Type alloy was observed by hot stage transmission electron microscopy, electron diffraction and motion picture micrography. Cold rolled and thinned polycrystalline foils were heated in situ and direct observation of oxide formation, types of oxides formed, mode of growth at different temperatures, growth rates and dynamic interaction with second phase particles were made.

As the foil was heated, oxidation occurred at several foil regions. The temperature for oxidation to commence at any region was sensitive to the amount of cold work introduced in the foil. The oxide formed was not a surface layer but proceeded through the entire foil thickness. The Al-Oxide interface movement was found to vary as a function of growth geometry, temperature change, and second phase particle interaction. The oxidation reaction

occurred close to equilibrium conditions and was reversible. Electron diffraction analysis showed the presence of two new types of oxides. Both these oxides could grow as an oriented layer in a (110) $\langle 221 \rangle$ fashion. At temperatures approaching the melting point of the matrix aluminum, oxidation occurred all over the surface by a spontaneous and irreversible process. At temperatures beyond the melting point of aluminum, there was neither a drastic change in the microstructure nor any sign of a continuous honeycomb network formation by alumina.

INTRODUCTION

Thermal transformation studies of aluminum and various alumina hydrates in oxidizing atmospheres yield a multitude of types of aluminum oxides. Some of these are crystalline, while others are close to being amorphous. In general, however, such studies have been confined to the oxidation of bulk single phase materials under high oxygen pressure. This has resulted in a fast oxidation reaction so that it has been possible to observe the reactants and products, but not the oxidation process as it occurred. Other investigators[1-3] have used the electron microscopy technique to study the oxidation of aluminum. In these investigations, the bulk aluminum foil was oxidized before being introduced into the microscope, so that only the surface oxide films have been examined in the microscope.

The present investigation was undertaken to observe the oxidation process as it occurred and, additionally, to study the effect of a distributed second phase and deformation structure on the subsequent oxidation of

a two-phase aluminum alloy.

Foils from an aluminum alloy containing a distributed aluminum oxide phase were cold rolled to various amounts and then thinned. They were then oxidized and concurrently observed by utilizing hot stage transmission electron microscopy. The foils were heated in situ and direct observation of oxide formation, types of oxides formed, mode of growth at different temperatures, growth rates and dynamic interaction with second phase particles were made. Sequential, stereo, selected area diffraction, high resolution diffraction and motion picture micrographs were taken as the foil was being heated. The ambient oxygen in the microscope column had a partial pressure around 10^{-4} torr. The resultant oxide growth rates were slow and occurred at an observable rate.

MATERIALS

The samples were fabricated by consolidating 3 μ diameter atomized aluminum powder by powder-metallurgical techniques. Spectroscopic analysis of the metal before atomizing showed the following composition:

Al....99.5 (min.) by difference			
Fe.... 0.25			
Si.... 0.10		Ga....	0.01
Cu.... 0.02		Mn....	<0.01
Zn.... 0.02		Mg....	<0.004

Atomizing decreases the aluminum content to about 98%, as each atomized particle is now coated with an oxide layer. The fabrication of this powder (designated AT-400) has been described elsewhere[4] in detail, and consists of cold pressing, vacuum sintering, hot pressing and hot extrusion to produce 1/4 inch diameter rods. During fabrication, the oxide coating on each of the aluminum particles breaks and gets distributed as irregular platelets in the aluminum matrix. The as-extruded rods were cold rolled to obtain 0.01 inch thick strips approximately 5/16 inch wide. These strips were recrystallized by annealing in air for about 8 hours at 1000°F. The material in this form was considered the bulk material for experimental purposes.

The structure of the recrystallized strips consists of irregular platelets of γ-Al_2O_3 (and possibly γ'-Al_2O_3) about 600 Å diameter and 150 Å thick, non-uniformly distributed in a commercial purity aluminum matrix.[4] The mean center-to center oxide spacing was less than 0.2 μ and the mean grain size around 500 μ.

EXPERIMENTAL

The recrystallized strips were reduced in thickness over the range 50% to 90% by cold rolling. Cold rolling leads to the development of a ragged cell structure, the cell size varying inversely with cold work.[5] A 90% cold rolled foil had a cell size of about 0.9μ. Thin foils less than 3000 Å thick, suitable for transmission electron microscopy were prepared using the "window" technique[6] from an electrolytic bath containing 20 volume per cent perchloric acid in absolute alcohol. The thinned foils were examined in a Hitachi HU-11B electron microscope operated at 100 kv and equipped with a combination tilt and rotation hot stage. Foils were heated inside the microscope from room temperature to temperatures above the melting point of aluminum. A typical heating curve is shown in Figure 1. On this curve, from O to A, the structure at room temperature was observed and micrographs were taken. At A the foil was heated. As the temperature was raised from A to B, oxidation did not occur, therefore no micrographs were taken in this range for this particular sample. At B, oxidation started to occur around etch pits. The temperature was held at B and micrographs taken during the time B to C. Temperature was again

increased, but nothing new happened until the point D was reached. At D, oxidation started to occur around the foil edge. Again the temperature was held at D and micrographs taken during the period DE. This process was continued until the temperature F was reached, which is above the melting point of aluminum. At this temperature, the foil started melting and broke at several irregular regions, having lost its mechanical strength. No further observation could therefore be made. Figure 1 is a curve for a particular foil. For another foil, the temperature at which oxidation occurs in a particular region may be above or below the temperatures shown in Figure 1. Thus, for this foil the heating curve would be similar in shape but would not coincide with Figure 1.

RESULTS AND DISCUSSION

The heating of the foils produced several distinctive structures in this alloy. These structures will be described and discussed separately.

Oxidation as Influenced by Deformation Structure:

As the foil is heated in situ, oxidation starts to occur successively at etch pits, at holes and edges, and then all over the surface. The temperature at which oxidation

starts to occur at any particular region is deformation sensitive. Table I gives the relation between per cent cold rolling and the temperature above which only oxidation would occur at a particular region. A larger deformation raises the temperature for oxidation to start at any region.

Mode of Oxidation:

During the electrothinning of the foil the voltage range is selected in such a way that the foil is attacked uniformly all over its surface. But conditions may vary from one foil region to another. Thus there may be regions where the local current density is high, leading to pitting. Figure 2 shows such an area, the pitted region appearing lighter in intensity. As the foils were heated, it was observed that such etch pits were the region where oxidation first occurred. For a 90% cold rolled foil, oxidation started to occur within the pitted regions at around 626°F. The oxidation process continued as the temperature was increased, but it proceeded beyond the etch pit boundary only above 900°F.

As the temperature is further increased, oxidation starts to occur around holes and foil edges. Holes are formed in a foil due to localized preferential polishing; e.g., at the second phase interfaces. Hence the periphery of such

TABLE I

Relation between Deformation Structure and Minimum Temperature for Oxidation to Occur at a Particular Region

Cold Rolling	Etch Pits	Holes and Edges	Nucleation by Second Phase γ-Al_2O_3	Throughout The Foil Surface
90%	626°F	660°F		0.86 Tm*
80%		600°F	780°F	0.86 Tm
50%		530°F		0.86 Tm

* Tm = Melting Point of Aluminum (1225°F)

holes is usually observed to contain projecting oxide particles (Figure 3). Figure 4 shows a 10 minute sequence at 760°F around a hole. Figure 5 shows the same area at a lower magnification. In all these figures identical particles have been assigned the same alphabet. Thus A is the same particle in Figures 4 and 5. Referring to Figure 4a, the white layer XYZ is the oxide (call it Oxide I) which started growing from the edge of the hole. Unlike the oxidation of pure aluminum previously reported,[3] this is not a surface layer but proceeds through the entire foil thickness. This has been confirmed by several stereo pairs (Figure 6).

The layer XYZ in Figure 4a, at the instant of formation, was a single phase appearing white in contrast. But within seconds, inside this layer another oxide (Oxide II) forms which appears as black particles (region around Y in Figure 4a). In Figure 4b, the boundary of Oxide I has, by sudden movement, thrown a loop to attain the configuration X'Y'Z'. At zero time the material inside this loop was entirely Oxide I. But in 10 minutes Oxide II particles have grown rapidly, the biggest particle being B' of diameter 360Å. Thus, for the reaction Oxide I → Oxide II, the fastest growth

rate is 36 Å/min.

By superimposing Figure 4b on Figure 4c, the mean lateral movement of the boundary X'Y' perpendicular to itself was also found to be 36 Å/min. That is, for the reaction Al → Oxide I, the fastest rate is also 36 Å/min. Thus the rate of forward movement of Oxide I equals the growth rate of Oxide II within the matrix of Oxide I. This suggests that at least at this temperature the reaction Al → Oxide I → Oxide II may occur close to equilibrium conditions, and may be written as Al ⇌ Oxide I ⇌ Oxide II. If this is true, then it should be possible to observe the reverse reaction; i.e., Oxide II → Oxide I, or the complete reaction Oxide II → Oxide I → Al, and/or Oxide II → Oxide I + Al. A large number of micrographs were taken, and it was observed that this reverse reaction is capable of taking place either completely or the first stage alone. The sequence in Figure 7 shows the first stage; i.e., Oxide II → Oxide I, occurring. In Figures 7a to 7d, particles A and B grow from Oxide I (white) around them until they meet each other (Oxide I → Oxide II). In Figure 7e, the reverse of this reaction occurs, so that the single particle of Oxide II in Figure 7d now breaks into two particles with Oxide I in between them (Oxide II → Oxide I).

The last stage of the reaction Oxide I → Al was rare.

Only one sequence in several dozens showed this (Figure 5). The particle A in Figure 5a has completely dissociated into Oxide I and Al (see Figure 5b). Here both stages of the reaction Oxide II → Oxide I → Al have occurred.

Note also that initially (Figure 7a) most of the regions around C consisted of Oxide I only, but with the lapse of time Oxide II particles started growing inside the matrix of Oxide I (Figure 7d) and continued to grow in Figure 7e. Thus, while the forward reaction is occurring in one region, the reverse reaction may also occur in an adjacent reaction, within a continuous Oxide I substrate. This is also shown by Figure 5, where a new region R containing Oxide I and Oxide II has appeared on one side (Figure 5b), while particle A (Figure 5a) has dissociated into Oxide I and Al on the other side. This again shows that these reactions occur close to equilibrium conditions.

Crystalline Form of Oxides I and II:

The diffraction patterns as well as the morphology of these oxides during growth (Figure 7c, particle A) suggest that they are indeed crystalline. Both selected area diffraction and high resolution diffraction studies were made in order

to identify the oxides. A standard gold foil was used at the beginning and end of every diffraction sequence to calculate the camera constant needed to solve these diffraction patterns. Figure 8 shows a typical high resolution diffraction micrograph, and Table II gives the spacing between the diffracting planes after deducting those due to aluminum.

In order to distinguish the spots coming from Oxide I from those of Oxide II, selected area diffraction of regions containing very small amounts of Oxide II (Figure 12c), and also areas containing large amounts of Oxide II (Figure 4c) were separately done. The results computed from several dozens of such micrographs after deducting those due to aluminum, are tabulated in Table III.

Oxide I could be assigned a pseudo F.C.C. lattice with a lattice parameter of 6.76 Å. Efforts to match the observed "d" values with the reported[1-3, 7-12] values of dozens of other Al_2O_3 failed. This was not surprising, since most of the reactions, $Al \rightarrow Al_2O_3$, mentioned in the literature were irreversible and the reported growth rates to form Al_2O_3 were much faster than observed in

TABLE II

Data for Oxide I and Oxide II

From High Resolution Diffraction Pattern

d(in Å)	I=Relative Intensity	d(in Å)	I=Relative Intensity
0.949	w	0.620	s
0.937	s	0.578	s
0.840	m	0.556	m
0.792	s	0.550	m
0.734	s	0.539	m
0.701	s	0.504	w
0.690	m	0.484	m
0.658	m	0.454	vw
0.629	m	0.436	w

Note: Intensity estimates are given with respect to oxide rings only. When compared to aluminum rings, the intensity of all the oxide rings are quite weak.

TABLE III

Data for Oxide I and Oxide II

from Selected Area Diffraction Pattern

a: Oxide I		b: Oxide II	
d(in Å)	I=Relative Intensity	d(in Å)	I=Relative Intensity
2.39	m	2.83	vvw
2.17	vvw	2.54	s
1.95	m	1.90	m
1.44	vvw		
1.38	m		

Note: Intensity estimates are given with respect to oxide spots only. When compared to aluminum spots, the intensity of all the oxide spots are very weak.

this investigation. Moreover, the conditions under which this study was conducted (e.g., an alloy containing a distributed oxide phase, matrix aluminum of commercial purity, heating in situ, low partial pressure of 0_2 atmosphere, faster heating rates), were much different from all these reported works. Considering this, it is probable that these are two new types of oxides not reported so far.

The Al- Oxide I Interface Movement:

In a preceding section, it was observed that the movement of the Al- Oxide I interface under isothermal conditions was slow (36 Å/minute) and more or less continuous. In this section the interface movement under athermal conditions will be described.

It was observed that if the temperature of the foil is suddenly increased, the Al- Oxide I interface moved by rapid, discontinuous steps. This was studied by taking motion pictures of the image of a heated specimen on the fluorescent screen in the electron microscope. In one such observation, the interface moved 1540 Å in 15 seconds by discontinuous jumps (rate of movement 6000 Å/minute) upon first heating to 850°F. Then the interface continued to grow in a slow but more uniform rate as the specimen reached constant temperature. The temperature was then suddenly raised to 880°F. During heating, the

interface again moved in a rapid, discontinuous manner proceeding 4100 Å in 10 seconds (25000 Å/minute).

Figure 9 shows a set of micrographs taken from this type of motion picture sequence. The motion pictures were taken when the foil was being heated, the temperature being in the range 570°F. Figure 9a shows two Oxide I layers, one growing from the foil edge marked E and the other growing from a hole marked H. A part of the two interfaces seem to be growing towards each other forming a U-shaped region. In Figure 9b, taken 1/12 second later, the interfaces have advanced toward each other and their forward edges now appear to be pointed in the shape of a V. The rate of advance from (a) to (b) was 2400 Å/second. In Figure 9c, taken 1/12 second after Figure 9b, the two interfaces have merged into each other so that a bridge shaped region marked R is formed. The rate of interface advance from (b) to (c) was 12000 Å/second. In Figure 9d, taken 90 seconds after Figure 9c, slow lateral growth of the bridge region has taken place (17 Å/second). Oxide II particles, marked S, have also grown in this bridge region. The largest of such particles was of diameter 1000 Å, corresponding to an Oxide II growth rate of at least 11 Å/second. Figure 9d also shows Oxide II particles marked P and Q have changed their morphology to a more geometric outline.

The above observations show that the Al- Oxide I interface movement varies as a function of growth geometry and temperature change.

Oriented Growth:

Oxide I grows in an oriented manner until "rapid oxidation" occurs (described later). This oriented growth is shown very clearly in Figure 10. This figure shows growth in two directions, OA and OB. On the other hand, Oxide II, which initially starts growing as discontinuous particles, may grow as an oriented layer at higher temperatures. Figure 11 shows such a sequence taken over a temperature range. Figure 11a shows oriented Oxide II growing in oriented Oxide I, the oriented growth direction being the same for both sides. As the temperature is increased, Oxide II becomes less oriented before Oxide I does (Figures 11b, c, d, e), but it still can grow as a continuous layer. During all these periods, discontinuous Oxide II particles continue to grow in the Oxide I matrix. Note that in Figure 3 the oxide perimeter does not appear to be oriented. This is because several layers grew from different holes. If the region around a single hole is considered, then it can be readily seen that it is indeed an oriented growth (region C, Figure 3).

Figure 12 contains sequences showing two oriented oxide layers meeting each other. Figure 12a contains a bi-crystal, with the boundary running along XYZ, and hence the diffraction pattern shows twin spots. Note also that Oxide I grows across the grain boundary of the matrix aluminum. The directions AB, AC (Figure 12c) were transferred to the corresponding selected area diffraction pattern (Figure 12d), taking into account the rotation due to the intermediate lens current. Actually, for our purpose the direction AB, corresponding to the plane of contact A'B' between oxide and metal, is of importance.* AB was then found to be the trace of (110) plane, and AC the trace of (221) plane. Therefore, the growth plane is (110) which is also the plane of contact between Al and Oxide I and the growth direction is $\langle 221 \rangle$. The lattice parameter for aluminum being 4.05 Å and for Oxide I being 6.76 Å, we can draw the plane of contact as shown in Figure 13.

Effect of γ-Al_2O_3 Particles in the Matrix:

a) Nucleation Effect. The intentionally added second phase γ-Al_2O_3 particles may, but need not, act as the nucleation site for Oxide I, but not for Oxide II. The

* We can assume that the planes whose traces are AB and AC are normal to the foil surface. This is a valid assumption since in several hundreds of micrographs taken, there was no evidence of any fringes along the oxide-metal boundary.

nucleated Oxide I could be oriented (region X,Y, Figure 3) or non-oriented (region R, Figure 14).

b) Dynamic Interaction with Oxide-Metal Interface. The moving oxide-metal boundary interacts with those dispersed second phase particles which protrude above the foil surface. This impeding effect is probably due to the beam and column contamination around these surface particles, acting as a mechanical barrier to oxygen, preventing it from reaching the oxidation interface. At C (Figure 4a), the oxide-metal interface interacts with several γ-Al_2O_3 particles and then bends to follow their contour. Individual particles (A, B, in Figure 15) can also obstruct the interface movement. Figure 10 shows second phase particles at the meeting points of two or more oxide boundaries. Obstructed by these particles, oxidation did not proceed smoothly and rectangular regions of aluminum have been left behind.

On the other hand, second phase particles wholly contained within the foil (B, Figure 4a), do not seem to offer such resistance.

Rapid Oxidation:

At approximately 0.86Tm temperatures, instead of an oxide layer growing slowly by progressive displacement of its interface, several irregular shaped areas throughout the foil surface

were rapidly oxidized. Figure 16 shows, at high magnification, the appearance of such areas (marked A) above the melting point of aluminum. These irregular areas rapidly meet each other (Figures 17a, b, c) to cover the entire foil surface.

Unlike the case of oxidation occurring along foil edges, here the entire foil surface is first covered with an oxide film. In the beginning, the layer is very thin, as the second phase γ-Al_2O_3 particles below this film are still visible (Figure 17). Then the film grows in thickness, becoming darker so that the structure below is not visible any more. Thus in this case the oxidation proceeds from the surface to the interior of the foil. Moreover, unlike the previous case, this oxidation process is spontaneous and irreversible. The γ-Al_2O_3 particles which project above the foil surface do not seem to impede its motion.

This oxide appears dark in contrast, due to the absorption of electrons from the beam. For this reason, no diffraction pattern could be obtained to find out whether it was a fast growing Oxide II or a different oxide structure.

There has been speculation[13] that alumina forms a continuous three-dimensional honeycomb skeleton within the aluminum matrix in SAP-Type alloys. Brammer and Dawe[14] observed a drastic change in microstructure above the melting

point of the matrix in a SAP alloy containing 4% Al_2O_3, and attributed this to a honeycomb network. These authors heated bulk samples of SAP-Type alloys for 25 hours at 1350°F in air. Being unable to prepare thinned samples from the bulk oxidized materials, the microstructure of the oxidized alloys was observed by optical metallography. In the present study when the foils were heated in situ beyond the melting point of aluminum, there was neither a drastic change in the microstructure, nor any signs of a honeycomb network formation of the second phase (Figure 16). It is also possible that during heating, γ-Al_2O_3 trapped within Oxide I may undergo phase transformation, as revealed by change in contrast of the individual particles (Figure 18, particles A). But unlike Brammer's observations, these transformation occurred below the melting point of the matrix.

Oxidation Mechanism:

During the preparation of the thinned foil, the foil surface is coated with a thin oxide layer. As the foil is heated inside the microscope, this oxide layer may prevent direct contact with ambient oxygen in the microscope column. It is not clear why oxidation should commence from the edge,

although due to the design of the instrument, the foil edge is less contaminated than the foil surface. Once oxidation starts from the edge, transfer of oxygen through this layer appears to be rate controlling. The slow rate of oxidation may be due to this effect, although the low partial pressure of oxygen atmosphere would also be expected to contribute towards this. The reversibility of the oxidation reaction, and in particular the reducing of the oxides to aluminum have never been observed before. Moreover, the oxidation and reduction reaction is capable of taking place simultaneously in two adjacent foil regions (Figure 5). This may be due to the presence of impurities in this alloy partitioning within the oxide phases, changing the activity of oxygen. Rapid Oxidation, as observed above, is not the same as Catastrophic Oxidation,[15] since the former process was not confined to any particular portion of the foil and occurred all over the surface as a layer. Considering the susceptibility of aluminum to oxidize, the latter process, if it were to take place, would have occurred much below the temperatures at which Rapid Oxidation was observed to occur.

The Oxide I boundary did not seem to interact with the deformation structure present in the matrix in which it is growing. The Oxide I boundary was observed to grow across matrix

grain boundaries without undergoing any change in orientation (Figure 12a). Moreover, the structure of oxides formed did not show any observable defect concentrations, either individual dislocations or dislocation networks. The growth direction of Oxide I and Oxide II seemed to be insensitive to the amount of deformation.

On the other hand, the deformation structure does seem to influence the temperature for oxidation to commence at any particular region in the foil. It may be mentioned that those foils which were cold rolled to a lesser degree, were thicker before being thinned. This variation in foil thickness with cold work may cause this apparent sensitivity of oxidation kinetics with the degree of rolling deformation.

CONCLUSIONS

The direct observation of the oxidation process as it occurs in a Al-2% Al_2O_3 polycrystalline SAP-Type alloy, has allowed the description of the oxidation process of a thin foil sample. The main features emergent from this investigation are as follows:

1. As the foil temperature is raised, oxidation occurs successively at etch pits, at holes and foil edge, and then all over the surface. The temperature for oxidation to commence at any foil region is sensitive to the deformation structure introduced in the foil. The oxidation rate is slow, and the oxide formed is not a surface layer but extends through the entire foil thickness.
2. Electron diffraction analysis showed the presence of two new types of oxides (Oxide I and Oxide II). Oxide I grows by progressive displacement of its interface. Oxide II grows inside Oxide I in the form of particles.
3. The Al → Oxide I → Oxide II reaction occurs close to equilibrium conditions and is reversible. The reverse reaction is capable of taking place either completely or in stages. Moreover, while the forward reaction is taking place in one foil region, the reverse reaction can occur simultaneously at an adjacent region.
4. The intentionally added second phase γ-Al_2O_3 may act as the nucleation site for Oxide I, but not for Oxide II. Those dispersed phase particles which

protrude above the foil surface seem to impede the moving Al-Oxide I interface. The second phase particles wholly contained within the foil do not seem to offer such resistance.

5. The Al- Oxide I interface movement varies as a function of growth geometry, temperature change and second phase particle interaction.

6. Oxide I grows oriented until "rapid oxidation" occurs. Oxide II may also grow oriented at higher temperatures, but as the temperature is further increased it becomes less oriented before Oxide I does. The growth orientation is (110) <221> for both the oxide types, and this is not influenced by prior cold work.

7. The Oxide I boundary did not appear to interact with the deformation structure present in the aluminum matrix. The structure of the oxides formed did not show any observable defect concentrations, either individual dislocations or dislocation networks.

8. At temperatures around 0.86 Tm, instead of an oxide growing slowly by progressive displacement of its interface, oxidation occurs from the surface to the

interior of the foil by a spontaneous and irreversible process.

9. As the foils were heated beyond the melting point of the aluminum matrix, there was neither a drastic change in the microstructure nor any sign of a continuous honeycomb network formation by alumina.

10. The γ-Al_2O_3 trapped within Oxide I may undergo phase transformation. These transformation seemed to occur below the melting point of the matrix.

ACKNOWLEDGEMENTS

The work reported in this paper was supported by both the National Aeronautics and Space Administration and the Office of Naval Research. The studies were conducted in the NASA Interdisciplinary Materials Research Center at Rensselaer Polytechnic Institute.

The authors wish to thank Drs. R. C. DeVries, Wim Veddar, B. R. Banerjee, Johann Joebstl and E. A. Leary for helpful discussions of some of the results. The authors express their deep appreciation to Mr. H. S. Kim for the preparation of extruded rods.

REFERENCES

1. J. M. Cowley, Acta Cryst., 6, 846 (1953)

2. I. S. Kerr, Acta Cryst., 9, 879 (1960)

3. K. Thomas and M. W. Roberts, J. Appl. Phys., 32, 70 (1961)

4. R. S. Goodrich and G. S. Ansell, Trans. Met. Soc. AIME, 230, 1372 (1964)

5. R. S. Goodrich and G. S. Ansell, Acta Met., 12, 1097 (1964)

6. R. B. Nicholson, G. Thomas and J. Nutting, Brit. J. Appl. Phys., 9, 25 (1958)

7. A.S.T.M. X-Ray Powder Data File

8. H. C. Stumpf, A. S. Russell, J. W. Newsome and C. M. Tucker, Ind. Eng. Chem., 42, 1398 (1950)

9. J. B. Newsome, H. W. Heiser, A. S. Russell, H. C. Stumpf, "Alumina Properties", Technical Paper No. 10, 2nd revision, Alcoa, Pittsburgh, 1960

10. M. K. B. Day and V. J. Hill, J. Phys. Chem., 57, 946 (1953)

11. R. Roy, V. G. Hill and E. F. Osborn, Ind. Eng. Chem., 45, 819 (1953)

12. Johann Joebstl, U. S. Army Engineering Research Development Laboratory, Fort Belvoir, Virginia, (private communication).

13. C. L. Myers and O. D. Sherby, J. Ins. Metals, 90, 380 (1962)

14. I. S. Brammer and D. W. Dawe, Technical Documentary Report, Contract AF 61(052)-463. October, 1964, Aeon Laboratories, Surrey, U. K.

15. Karl Hauffe, Oxidation of Metals, Plenum Press, New York, 1965, pp. 5-6, 248-250

FIGURE CAPTIONS

Figure 1 Typical *in situ* heating curve for a 90% cold rolled foil.

Figure 2 Etch pits in a 90% cold rolled foil. Black particles are intentionally added γ-Al_2O_3 particles.

Figure 3 Holes (marked H) in a 90% cold rolled foil, heated to 1050°F *in situ*. The white region (marked A) around holes is Oxide I. The grey region (marked B) is aluminum. Black particles are γ-Al_2O_3.

Figure 4 Region around a hole containing Oxide I and Oxide II in a 90% cold rolled foil heated to 760°F.

- 4a At zero time
- 4b 10 minutes from (a)
- 4c 10 minutes from (b)

Figure 5 Same region as shown in Figure 4 at lower magnification. H is the hole. Temperature=760°F.

- 5a At zero time
- 5b 15 minutes from (a)

Figure 6 A stereo pair showing Oxide I and Oxide II growing in the aluminum matrix. E is the foil edge. γ-Al_2O_3 particles are marked A, and Oxide II particles are marked B.

Figure 7 A 90% cold rolled foil heated to 1015°F. A and B are Oxide II particles. H is a hole in the foil. C is the Oxide I layer and D is the aluminum matrix.

- 7a At zero time
- 7b 15 seconds from (a)

7c 15 seconds from (b)
7d 15 seconds from (c)
7e 10 seconds from (d)

Figure 8 High resolution diffraction micrograph of a polycrystalline cold rolled and oxidized sample showing rings from aluminum, Oxide I and Oxide II.

Figure 9 Motion picture sequence of an 80% cold rolled sample taken at 570°F.

9a At zero time
9b 1/12 second after (a)
9c 1/12 second after (b)
9d 90 seconds after (c)

Figure 10 Oriented growth in a 58% cold rolled sample at 666°F.

Figure 11 Oriented Oxide I and Oxide II growth in a 90% cold rolled foil.

11a Temperature 850°F
11b 14 minutes from (a), temperature 930°F.
11c 9 minutes from (b), temperature 990°F.
11d 8 minutes from (c), temperature 1050°F.
11e 9 minutes from (d), temperature 1100°F

Figure 12 Oriented Oxide I layers meeting each other in a 90% cold rolled foil at 840°F

12a At zero time
12b 10 seconds from (a)
12c 20 seconds from (b)
12d Selected area diffraction pattern of the region shown in (c)

Figure 13 Schematic of the (110) plane of Al and Al_2O_3

Figure 14 Non-oriented nucleation by second phase particles in an 80% cold rolled foil heated to 780°F. E is the foil edge

Figure 15 Individual γ-Al_2O_3 particles impeding interface movement in an 80% cold rolled foil. Temperature 1030°F.

Figure 16 Areas (marked A) undergoing rapid oxidation in a 90% cold rolled foil. Temperature 1250°F.

Figure 17 Oxide patches formed during rapid oxidation in a 90% cold rolled foil at 1050°F.

17a At zero time
17b 15 seconds from (a)
17c 15 seconds from (b)

Figure 18 A split second micrograph showing a part of individual oxide particles (marked A) changing contrast. Foil 80% cold rolled, temperature 1030°F

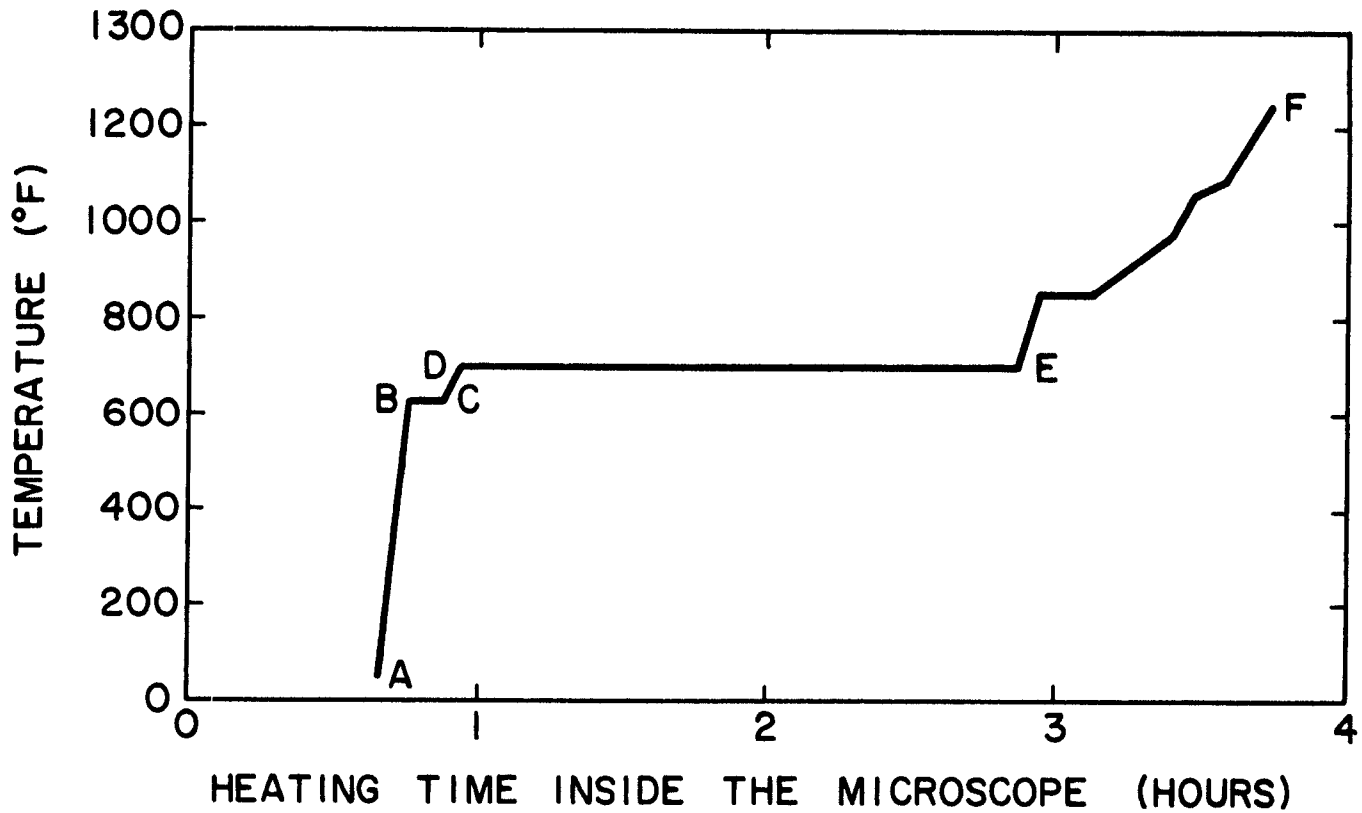
1300
1200
1000
800
600
400
200
0
TEMPERATURE (°F)
A
B
C
D
E
F
0
1
2
3
4
HEATING TIME INSIDE THE MICROSCOPE (HOURS)

FIGURE 1.

FIGURE 2

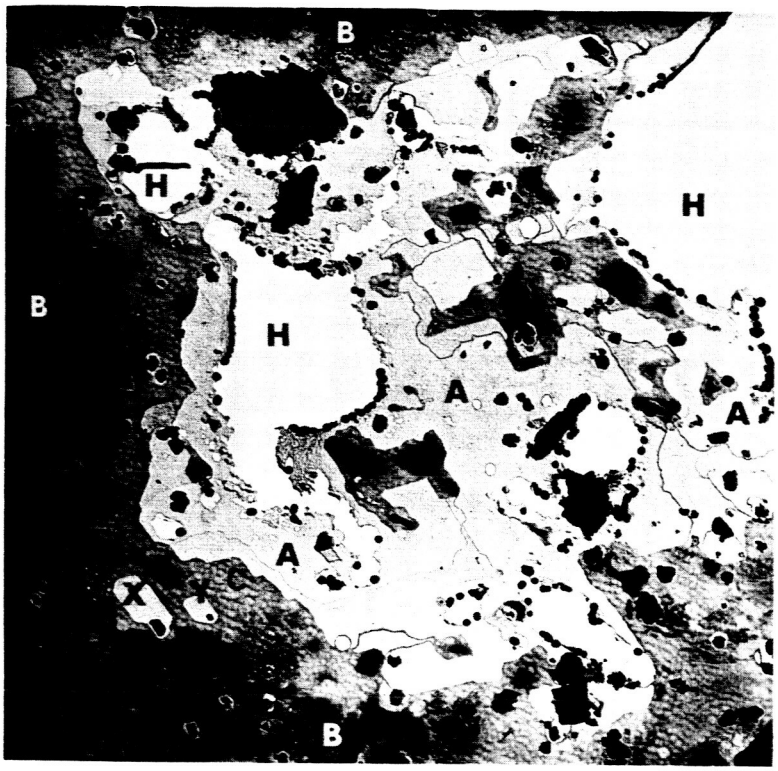

FIGURE 3

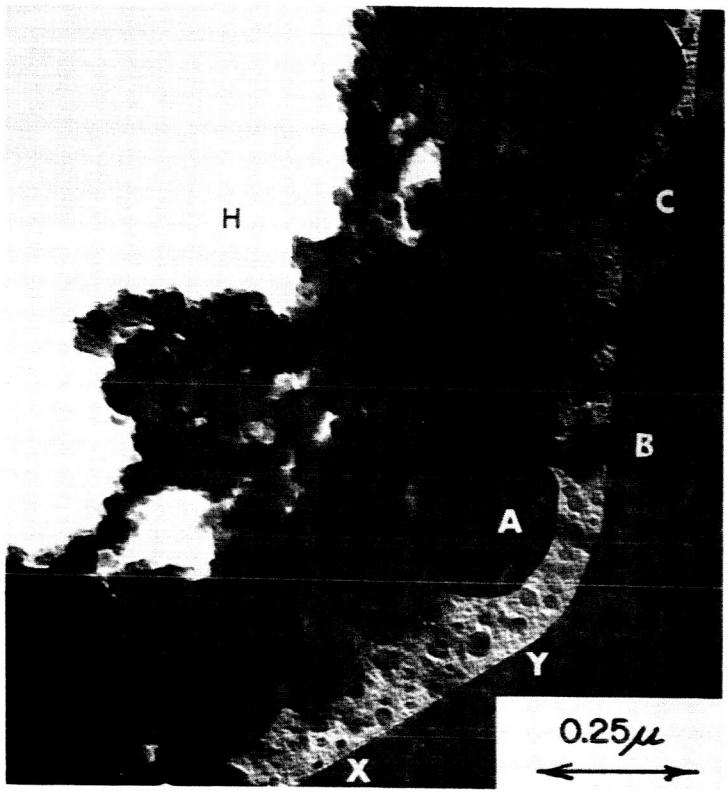

a

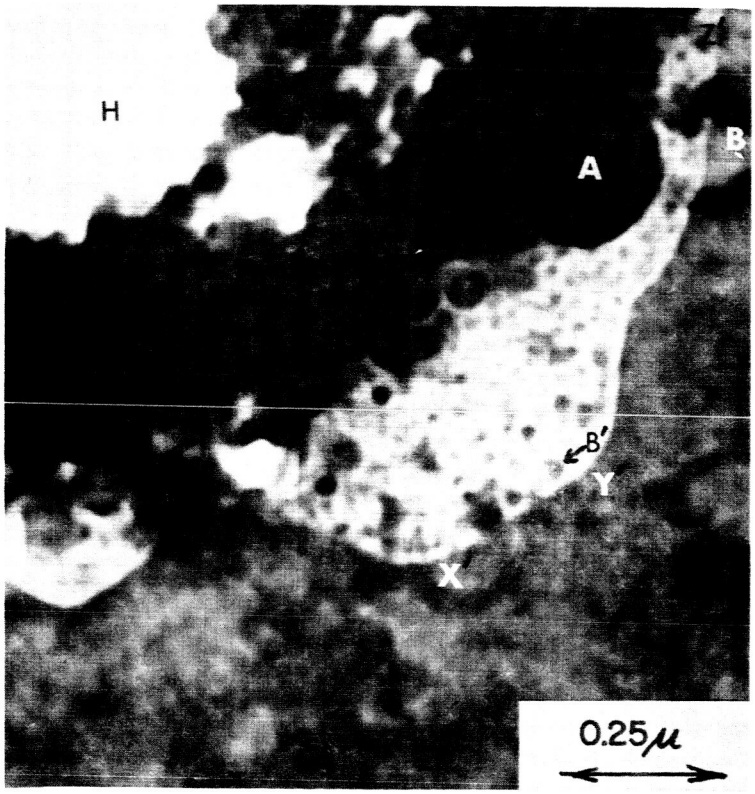

b

FIGURE 4

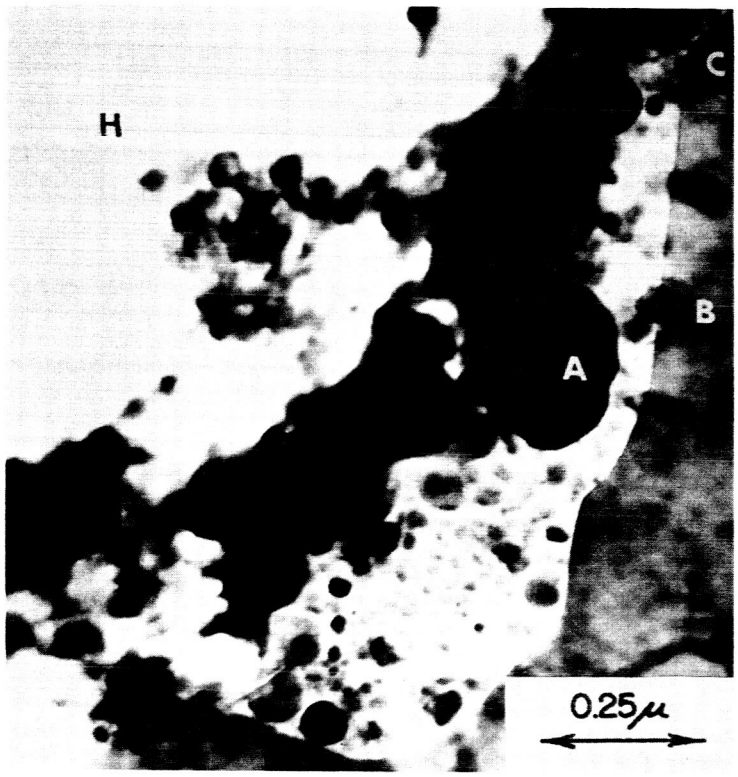

c

FIGURE 4

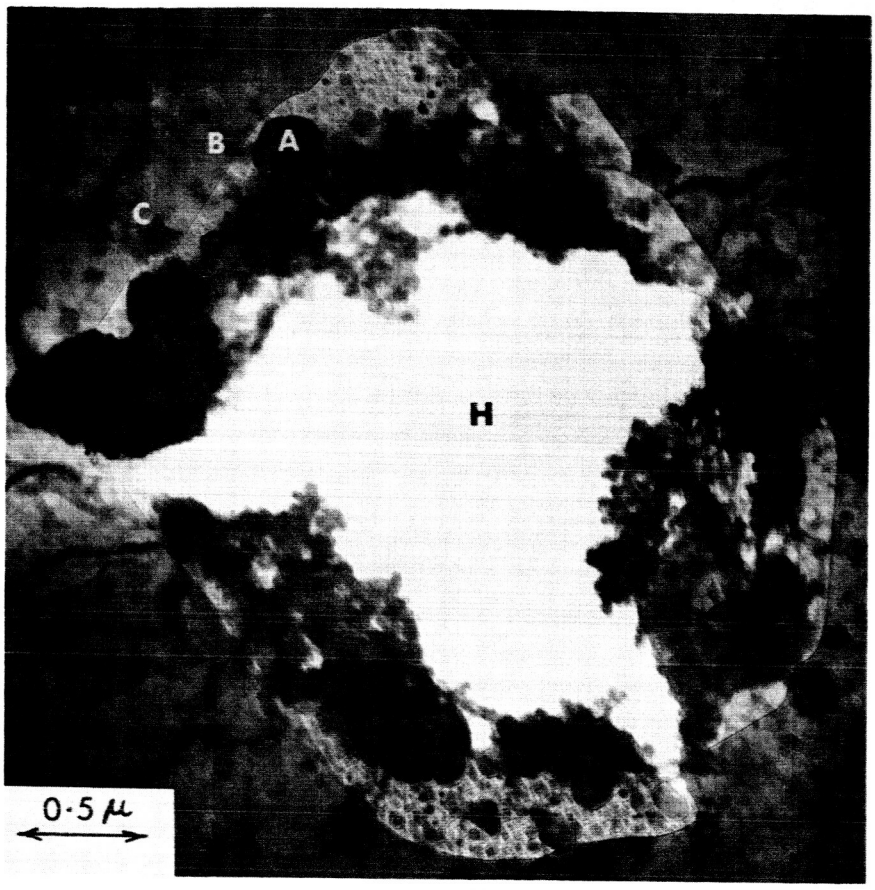

a

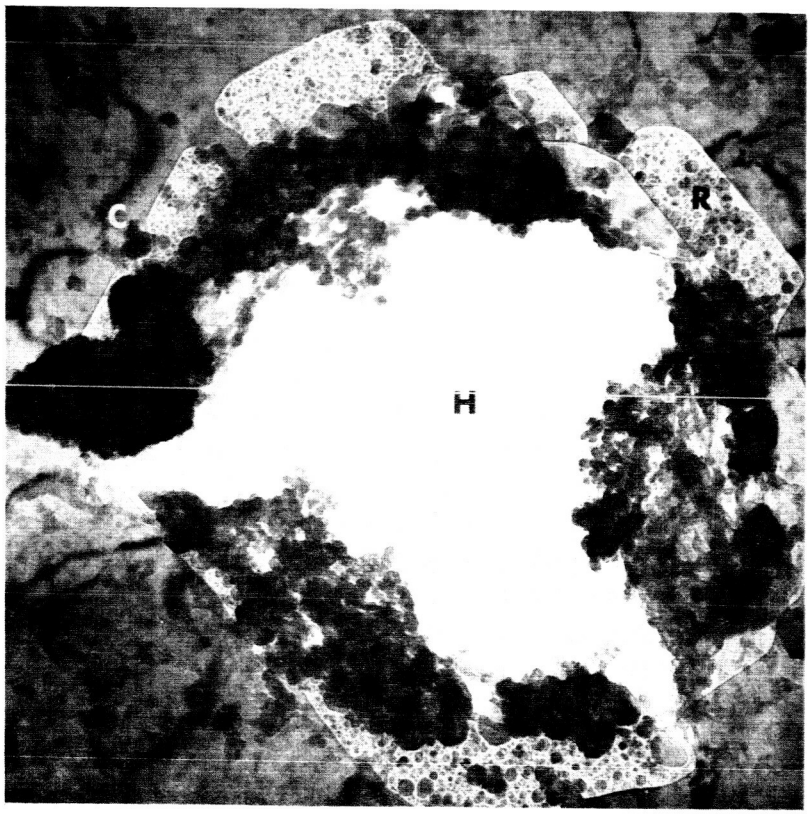

b

FIGURE 5

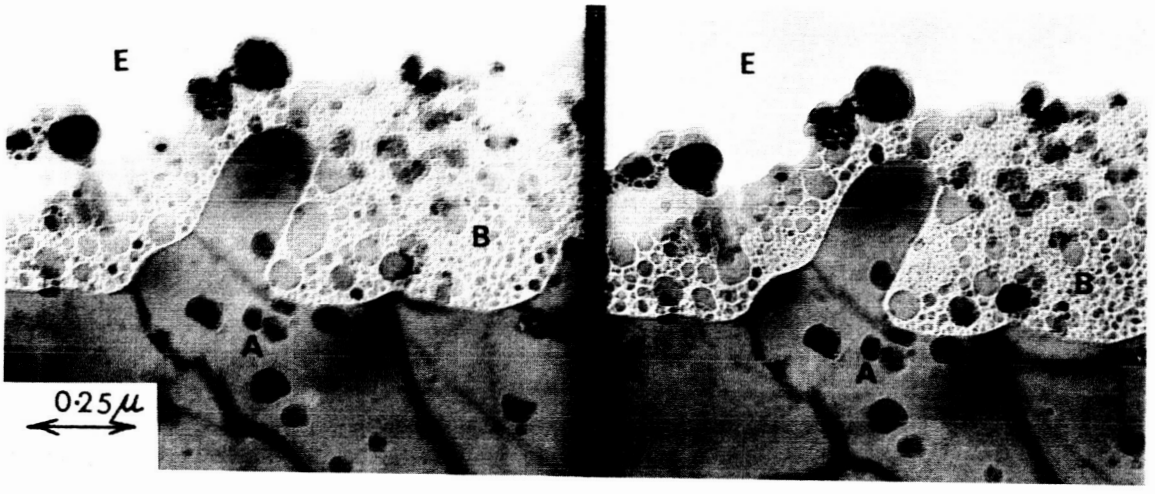

FIGURE 6

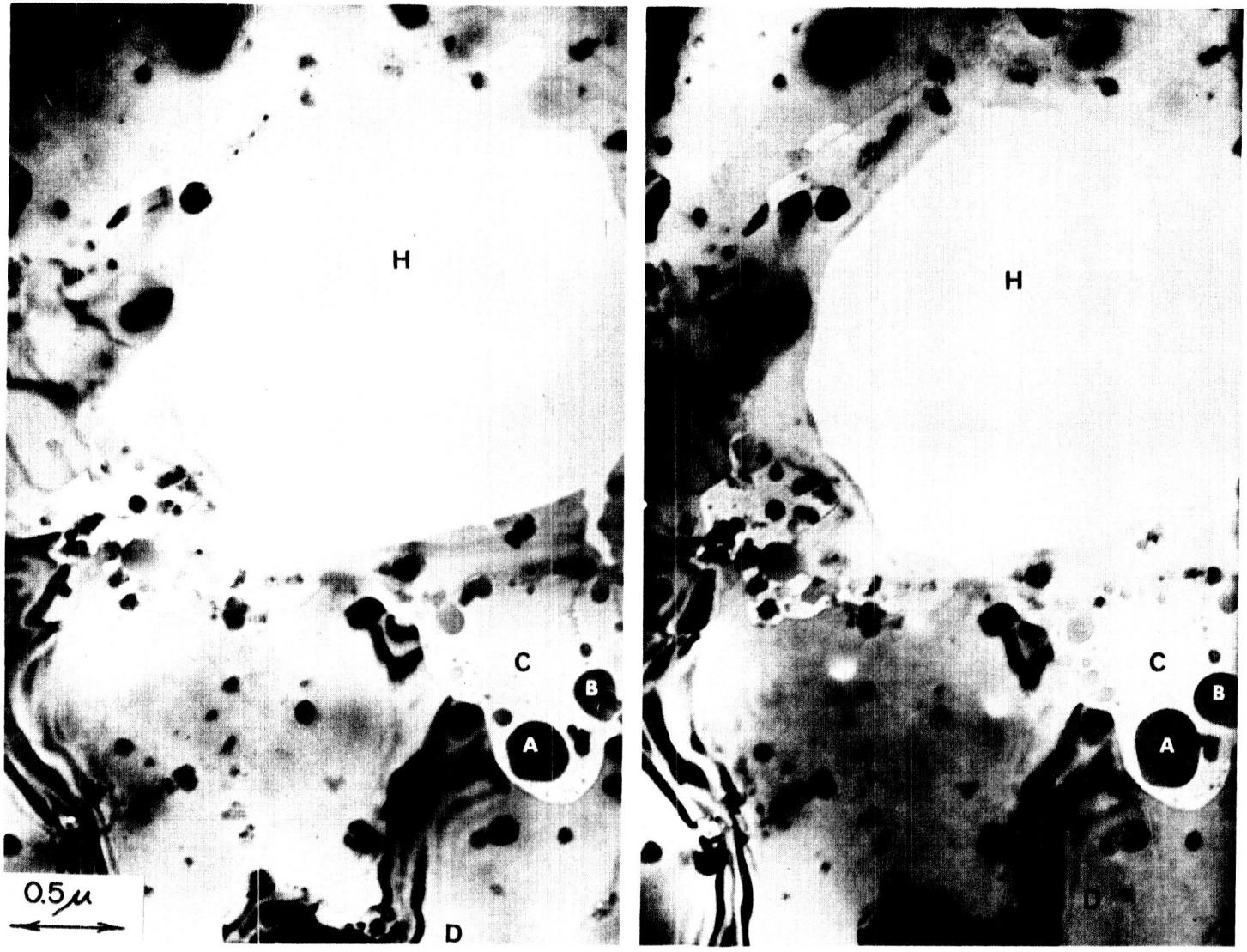

FIGURE 7

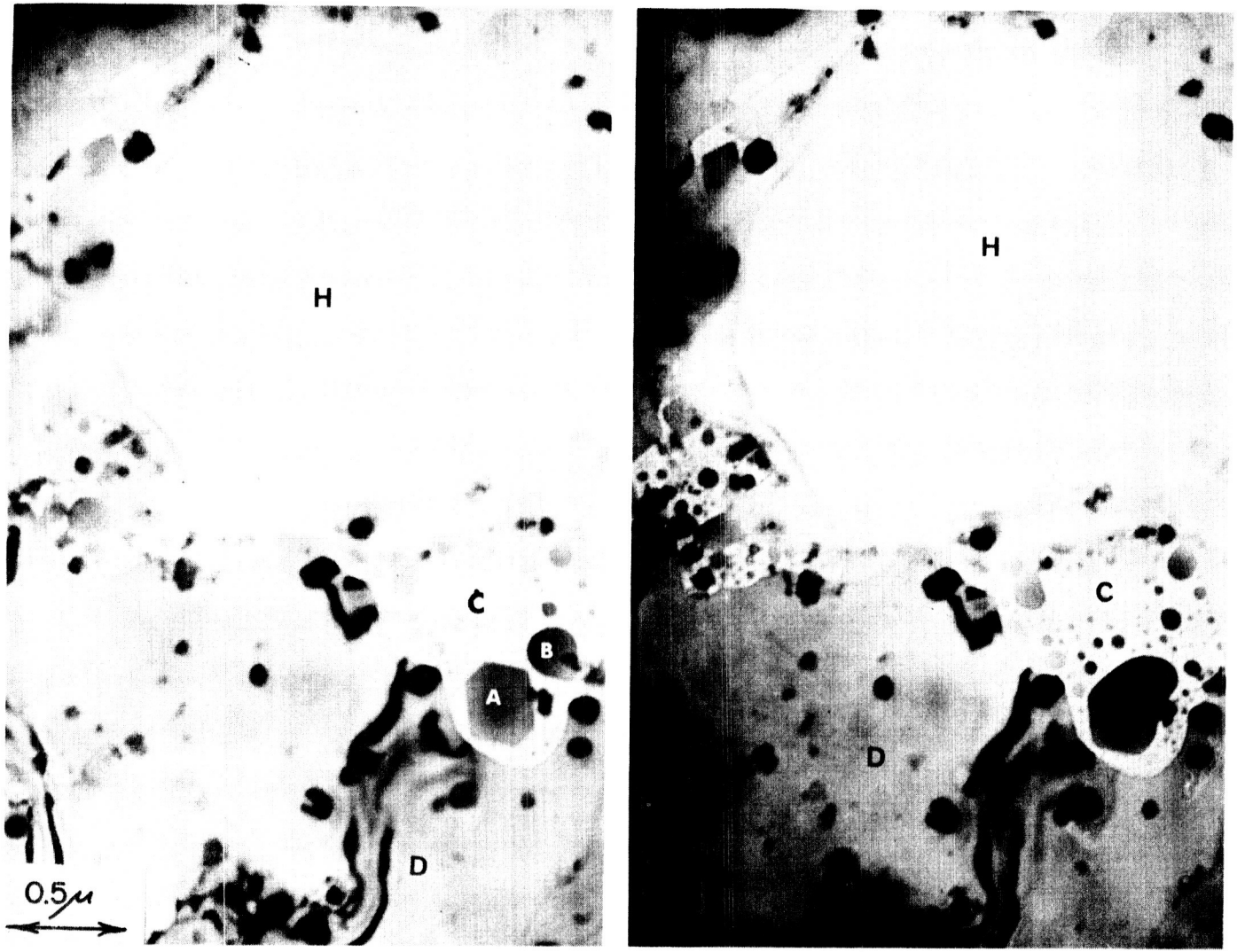

FIGURE 7

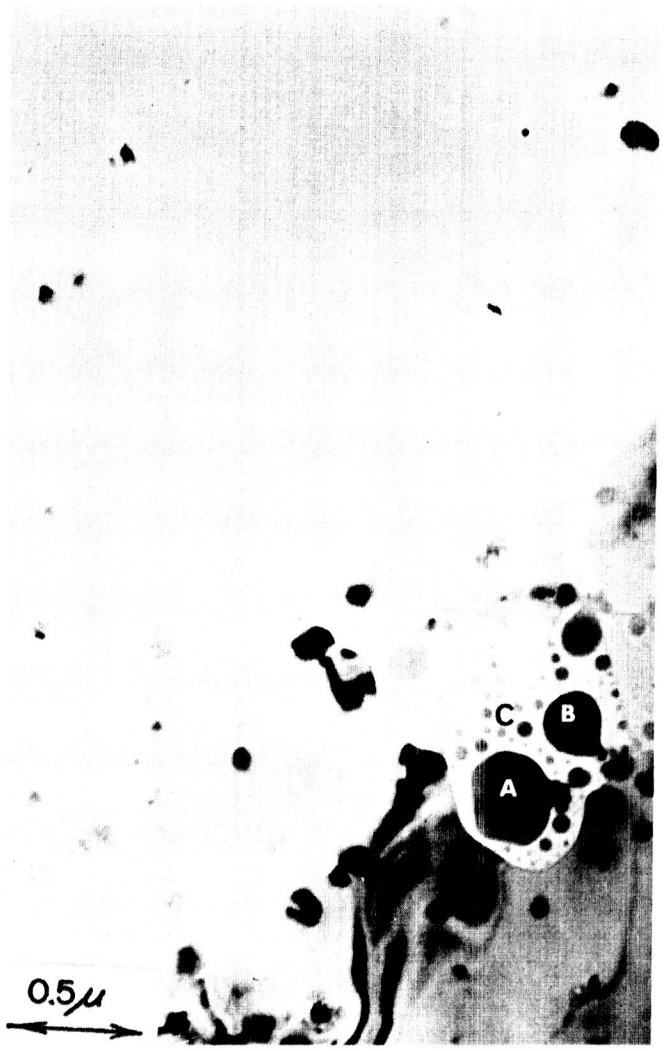

e

FIGURE 7

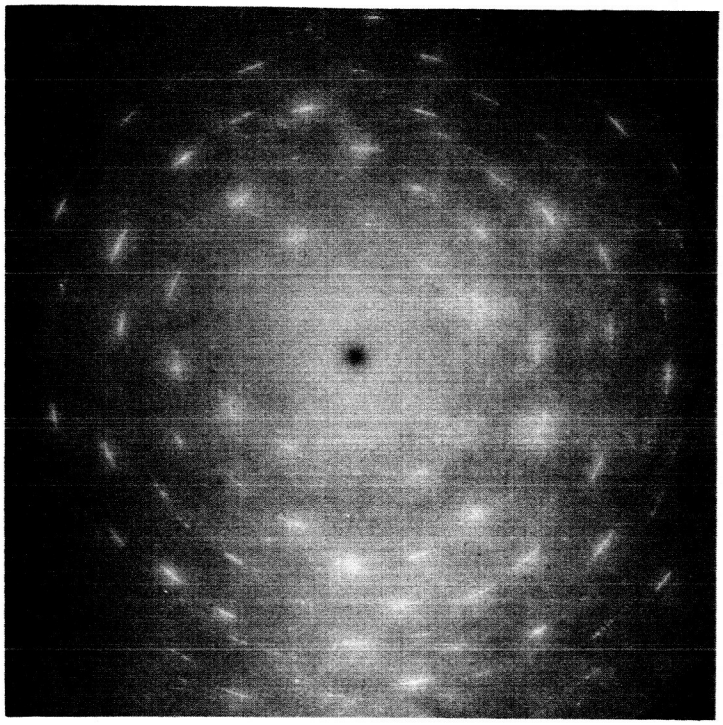

FIGURE 8

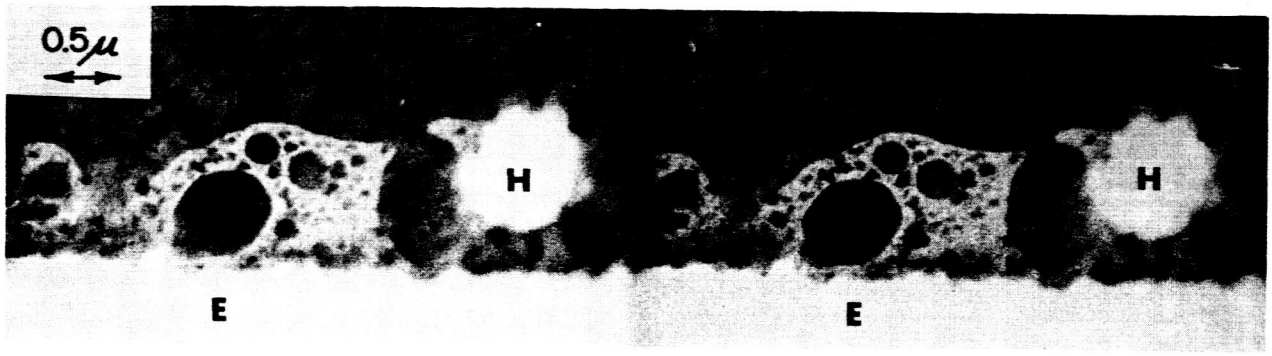

a b

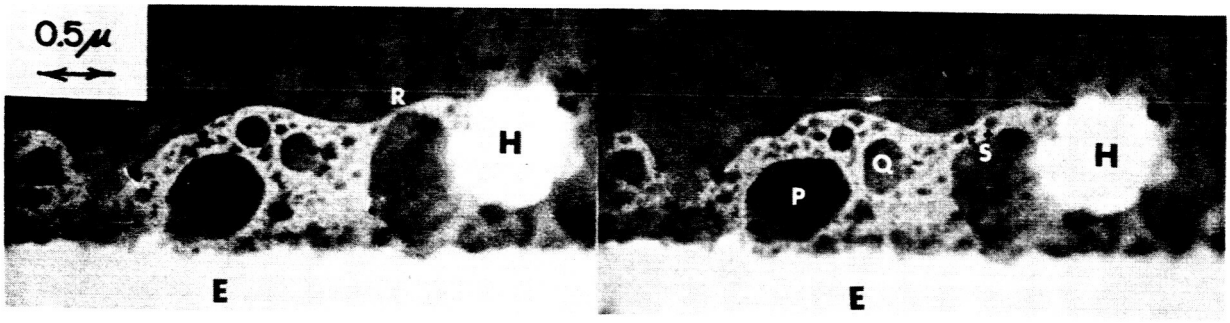

c d

Figure 9

Figure 10

a

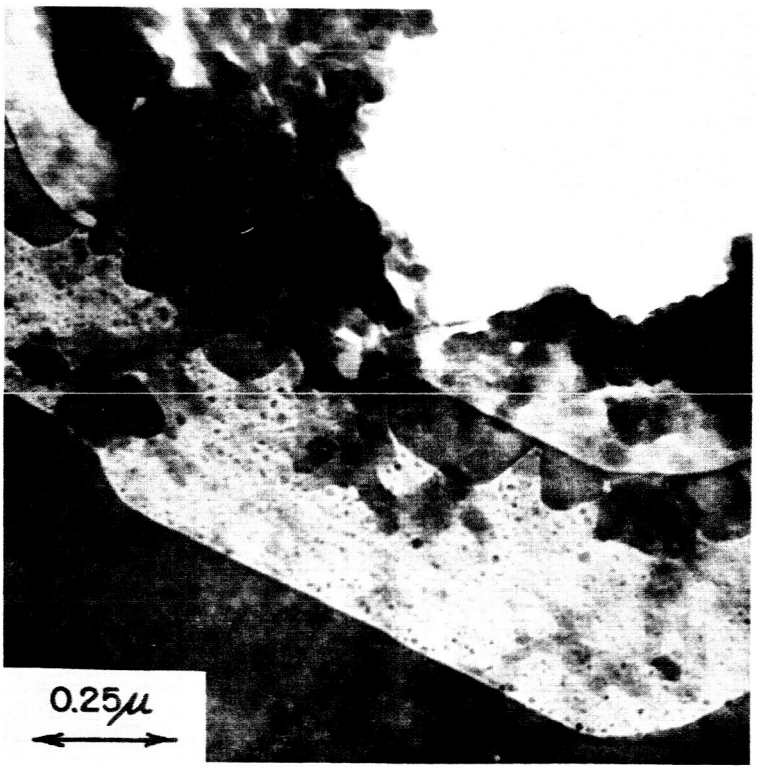

b

Figure 11

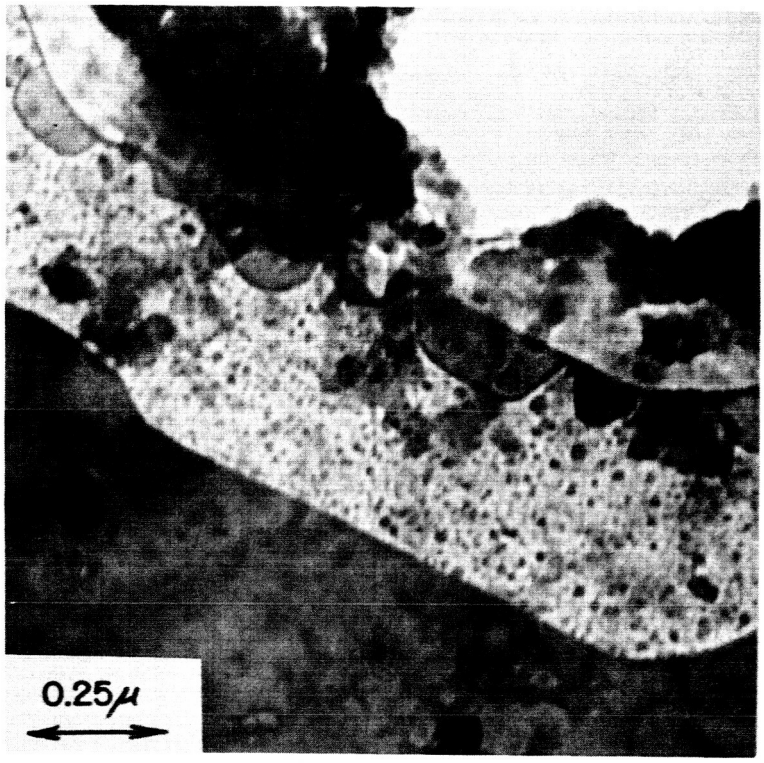

c

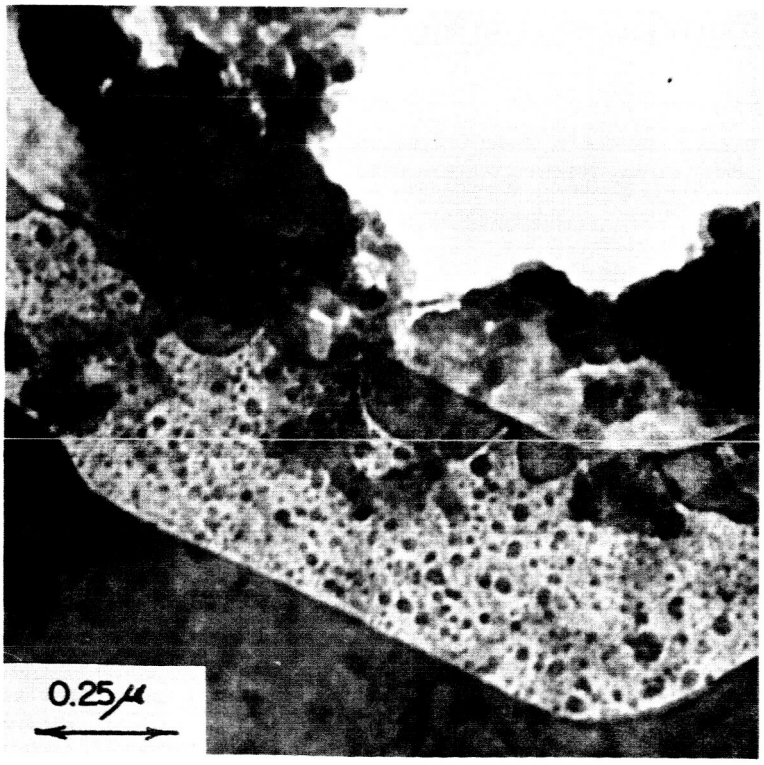

d

Figure 11

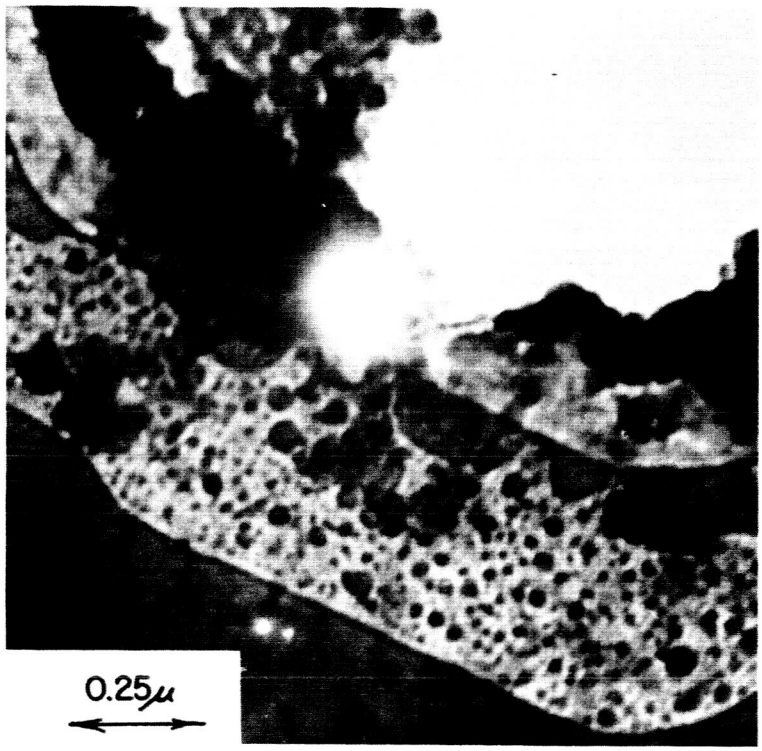

e

Figure 11

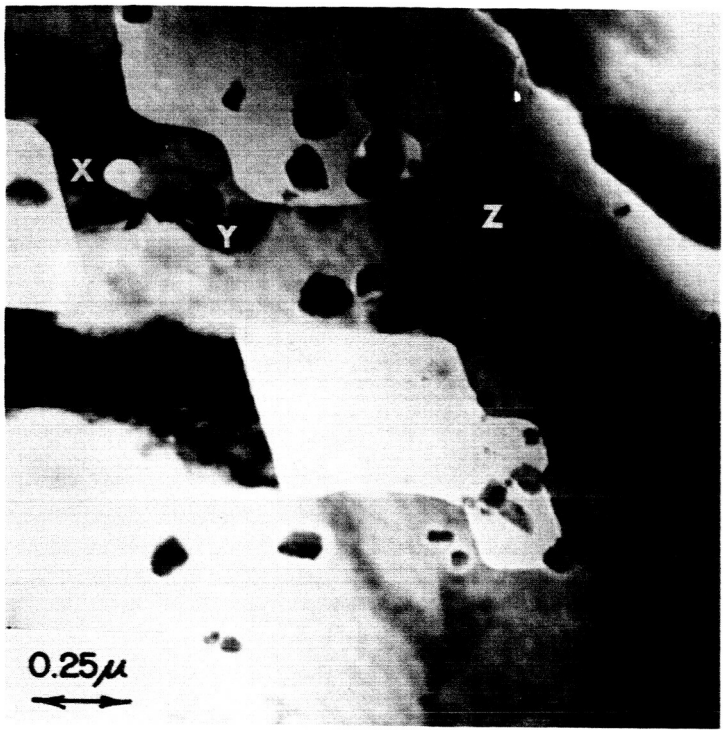

a

b

Figure 12

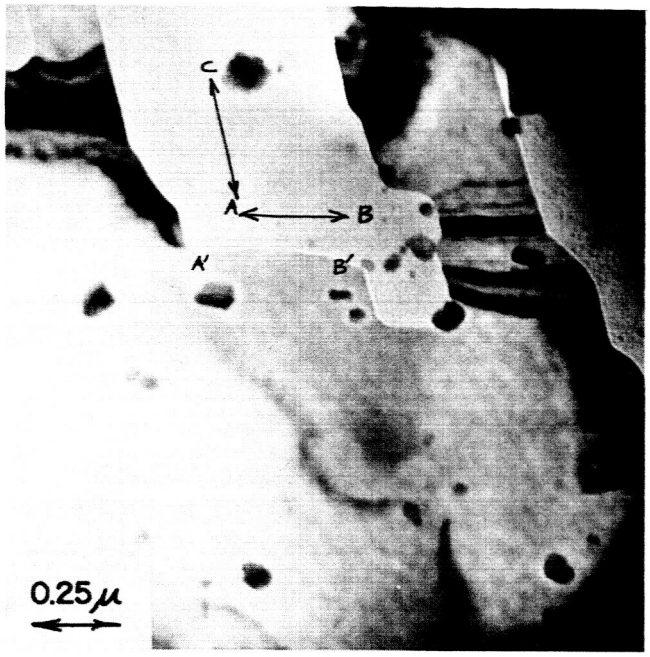

c

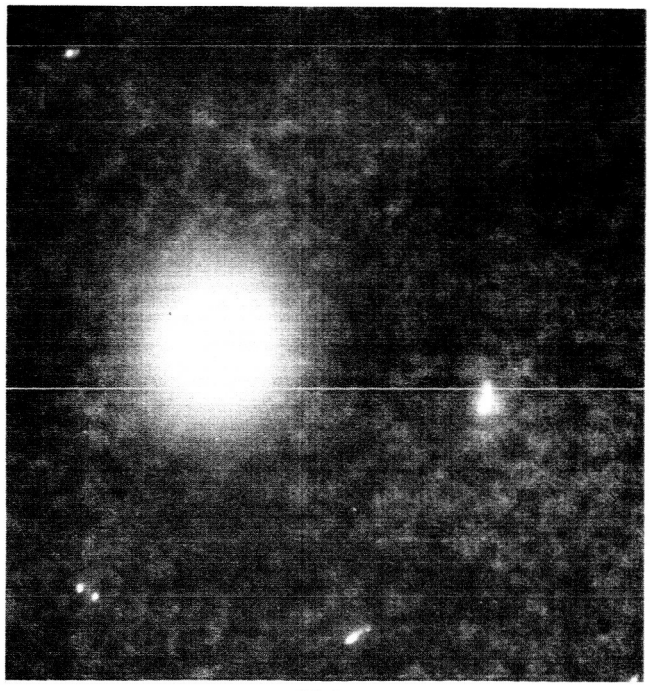

d

Figure 12

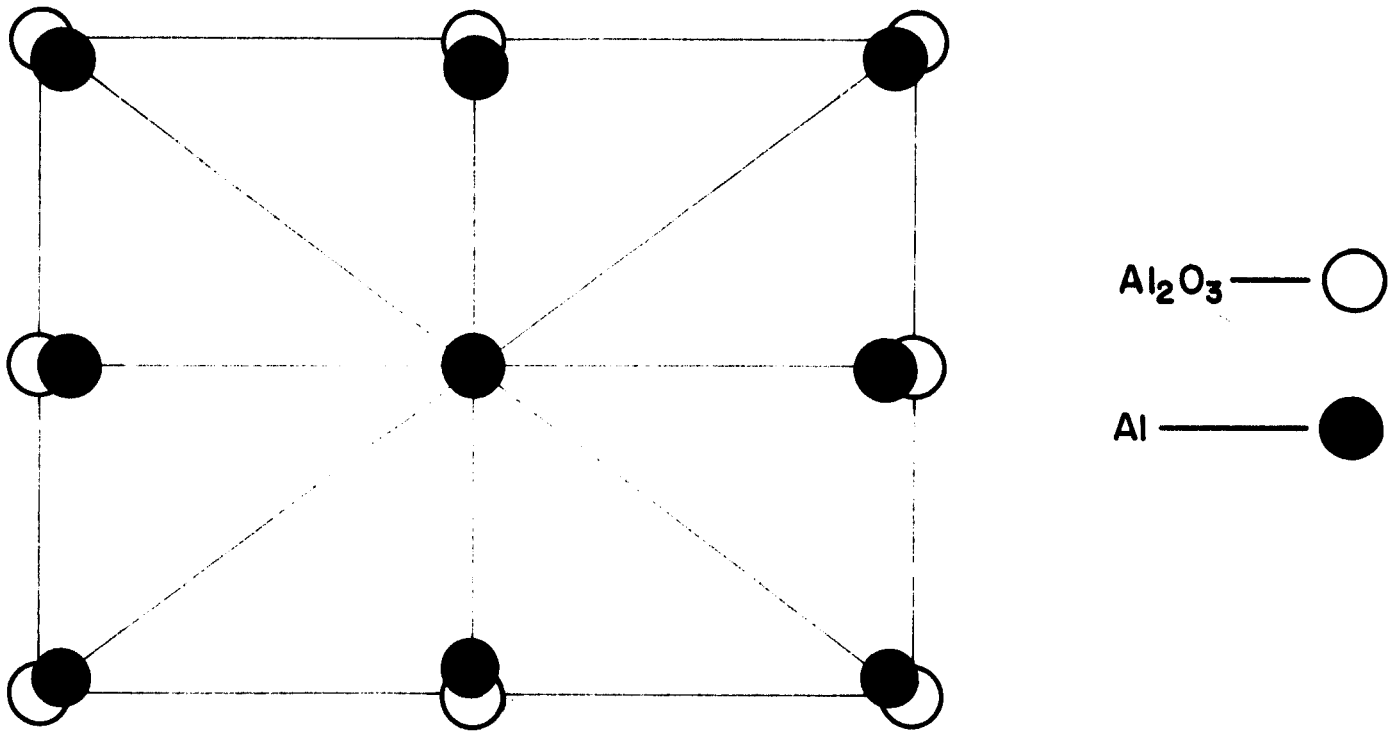

FIGURE 13.

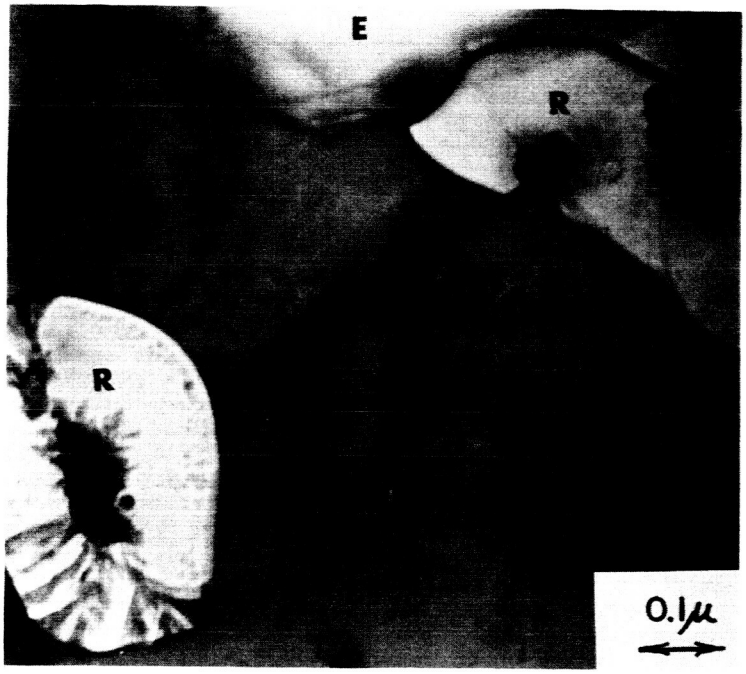

Figure 14

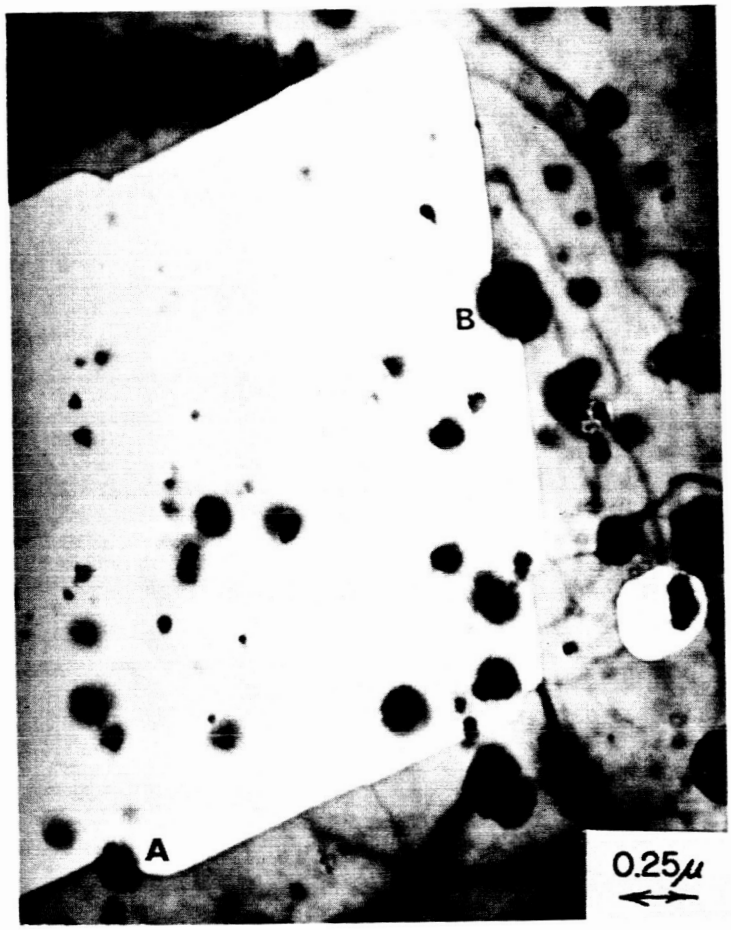

Figure 15

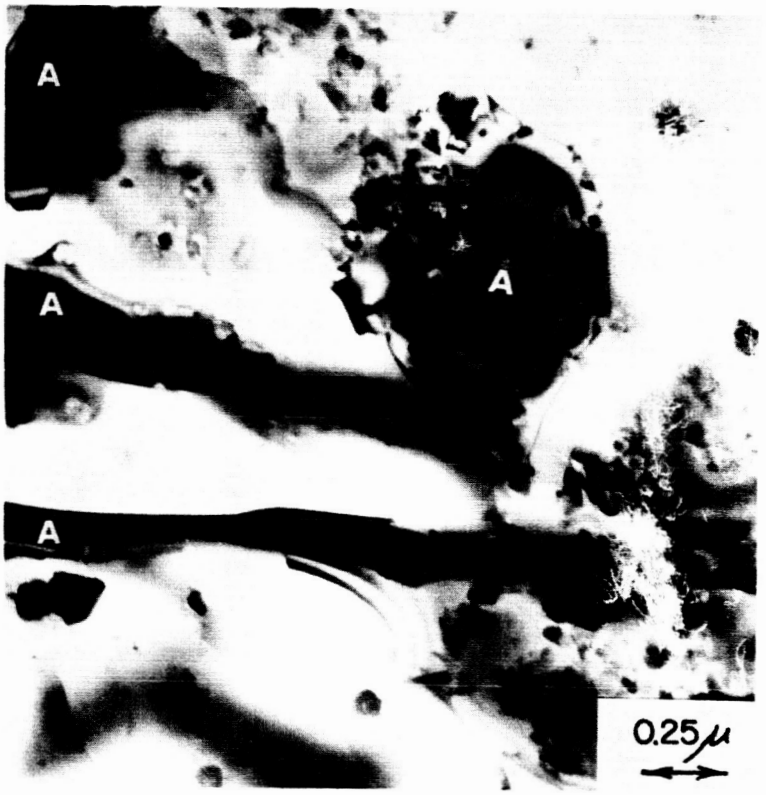

Figure 16

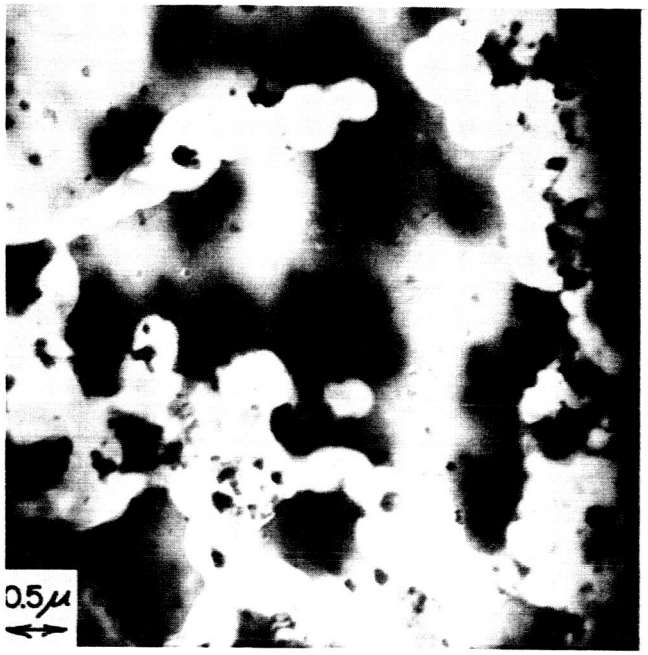

a

b

Figure 17

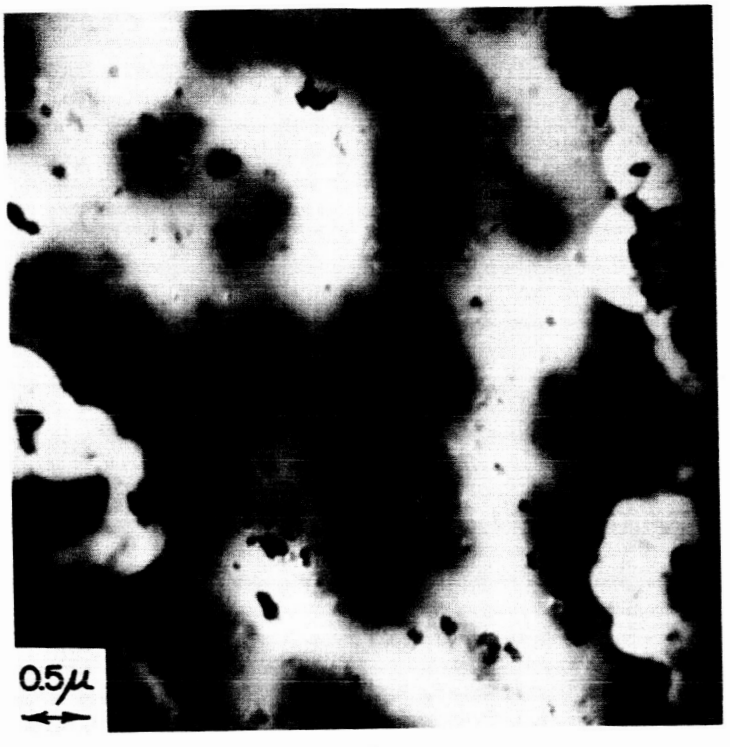

c

Figure 17

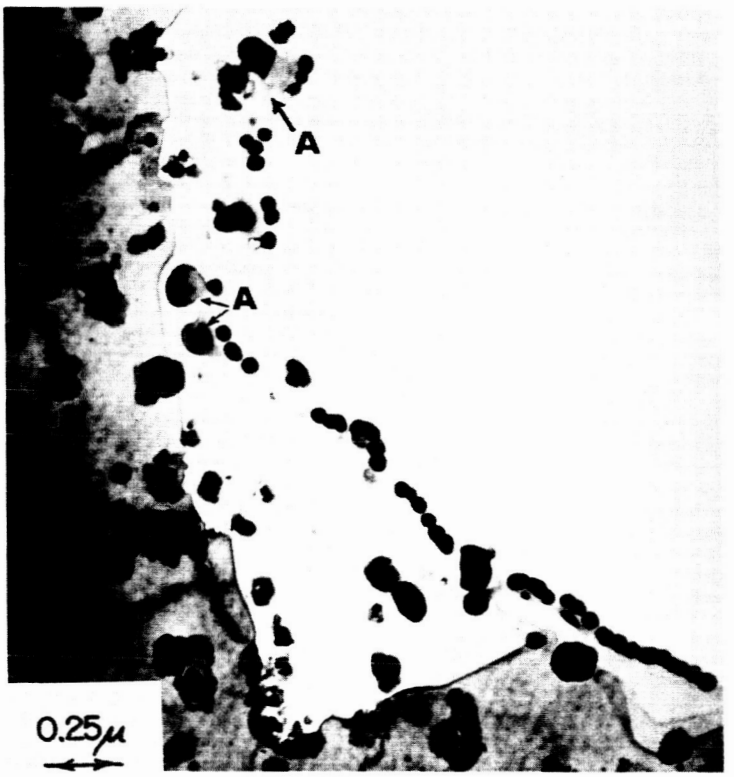

Figure 18